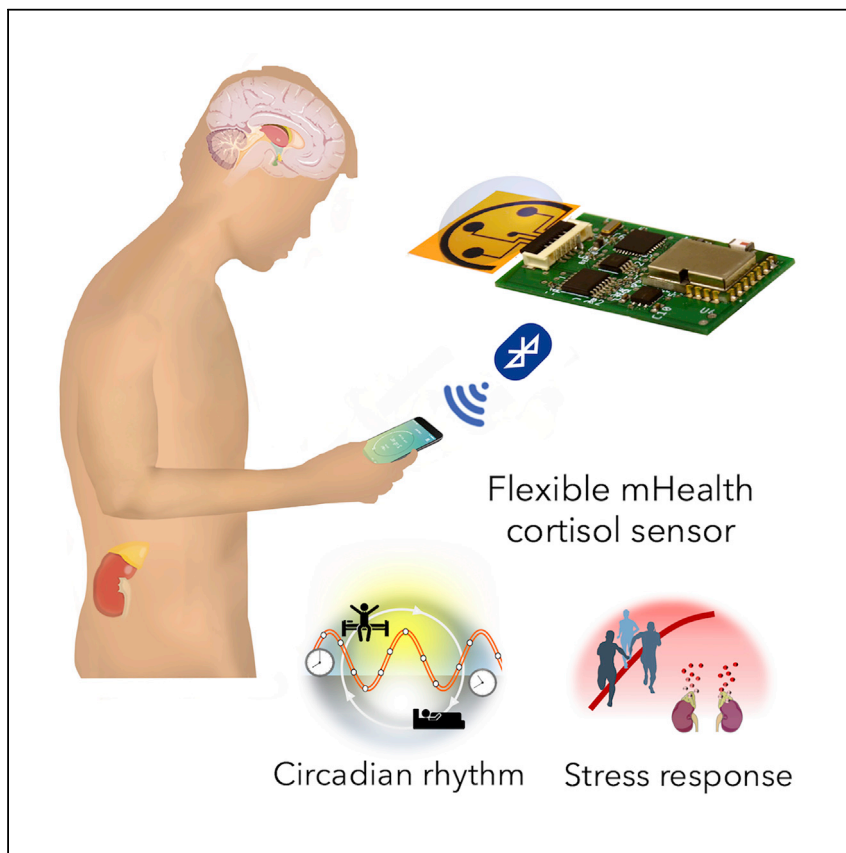


## Article

# Investigation of Cortisol Dynamics in Human Sweat Using a Graphene-Based Wireless mHealth System



Rebeca M. Torrente-Rodríguez, Jiaobing Tu, Yiran Yang, ..., Cui Ye, Waguih William IsHak, Wei Gao

weigao@caltech.edu

## HIGHLIGHTS

A fully integrated, flexible, and wireless device for sweat cortisol monitoring

Mass-producible graphene sensor array for sensitive and reliable measurements

A strong correlation between serum and sweat cortisol is obtained

The diurnal cycle and stress-response profile of sweat cortisol are reported

A fully integrated, flexible, and miniaturized wireless mHealth sensing device based on laser-engraved graphene and immunosensing with proven utility for fast, reliable, sensitive, and non-invasive monitoring of stress hormone cortisol is developed. Pilot human study results revealed a strong correlation between sweat and circulating hormone for the first time. Both cortisol diurnal cycle and dynamic stress-response profiles were established from human sweat, reflecting the potential of such mHealth devices in personalized healthcare and human performance evaluation.



## Understanding

Dependency and conditional studies on material behavior

Torrente-Rodríguez et al., Matter 2, 921–937  
April 1, 2020 © 2020 Elsevier Inc.  
<https://doi.org/10.1016/j.matt.2020.01.021>



## Article

# Investigation of Cortisol Dynamics in Human Sweat Using a Graphene-Based Wireless mHealth System

Rebeca M. Torrente-Rodríguez,<sup>1,3</sup> Jiaobing Tu,<sup>1,3</sup> Yiran Yang,<sup>1</sup> Jihong Min,<sup>1</sup> Minqiang Wang,<sup>1</sup> Yu Song,<sup>1</sup> You Yu,<sup>1</sup> Changhao Xu,<sup>1</sup> Cui Ye,<sup>1</sup> Waguih William IsHak,<sup>2</sup> and Wei Gao<sup>1,4,\*</sup>

## SUMMARY

Understanding and assessing endocrine response to stress is crucial to human performance analysis, stress-related disorder diagnosis, and mental health monitoring. Current approaches for stress monitoring are largely based on questionnaires, which could be very subjective. To avoid stress-inducing blood sampling and to realize continuous, non-invasive, and real-time stress analysis at the molecular levels, we investigate the dynamics of a stress hormone, cortisol, in human sweat using an integrated wireless sensing device. Highly sensitive, selective, and efficient cortisol sensing is enabled by a flexible sensor array that exploits the exceptional performance of laser-induced graphene for electrochemical sensing. Here, we report the first cortisol diurnal cycle and the dynamic stress-response profile constructed from human sweat. Our pilot study demonstrates a strong empirical correlation between serum and sweat cortisol, revealing exciting opportunities offered by sweat analysis toward non-invasive dynamic stress monitoring via wearable and portable sensing platforms.

## INTRODUCTION

The exponential increase in the pace of life in the 21<sup>st</sup> century constantly demands intense and prolonged mental as well as physical efforts from individuals,<sup>1</sup> both of which are potential triggers of stress. Chronic stress has been associated with higher risks of anxiety, depression, suicide, and weakening immune response, as well as cardiovascular diseases.<sup>2</sup> The need for measurable stress indicators has never been more than apparent, be it in the contexts of post-traumatic stress disorder (PTSD) screening and depression evaluation, or a more general mental and somatic health monitoring setting. Although psychosocial and physiological stresses are induced by distinct stimuli, they share similar neuroendocrine and behavioral responses regulated by the hypothalamic-pituitary-adrenal (HPA) axis.<sup>3</sup> Activation of the HPA axis stimulates the secretion of glucocorticoids (e.g., cortisol), a group of hormones that mobilize energy in the body to cope with stress (Figure 1A).<sup>4</sup> While short-term alterations in the HPA axis are deemed as normal and adaptive responses of the body, chronic dysregulation of the HPA axis, an energetically costly state, is associated with various pathological processes. As such, stress and individuals' stress-coping responses are perceived as dynamic processes; absolute quantification of stress level provides much richer information and greater diagnostic value in the context of time and environment.<sup>5</sup>

Experience sampling methods such as questionnaires and diary studies play a pivotal role in establishing the situational contexts of stressors in relevant

## Progress and Potential

Prompt and accurate detection of stress is essential to the monitoring and management of mental health and human performance. Considering that current methods such as questionnaires are very subjective, we propose a highly sensitive, selective, miniaturized mHealth device based on laser-enabled flexible graphene sensor to non-invasively monitor the level of stress hormones (e.g., cortisol). We report a strong correlation between sweat and circulating cortisol and demonstrate the prompt determination of sweat cortisol variation in response to acute stress stimuli. Moreover, we demonstrate, for the first time, the diurnal cycle and stress-response profile of sweat cortisol, revealing the potential of dynamic stress monitoring enabled by this mHealth sensing system. We believe that this platform could contribute to fast, reliable, and decentralized healthcare vigilance at the metabolic level, thus providing an accurate snapshot of our physical, mental, and behavioral changes.



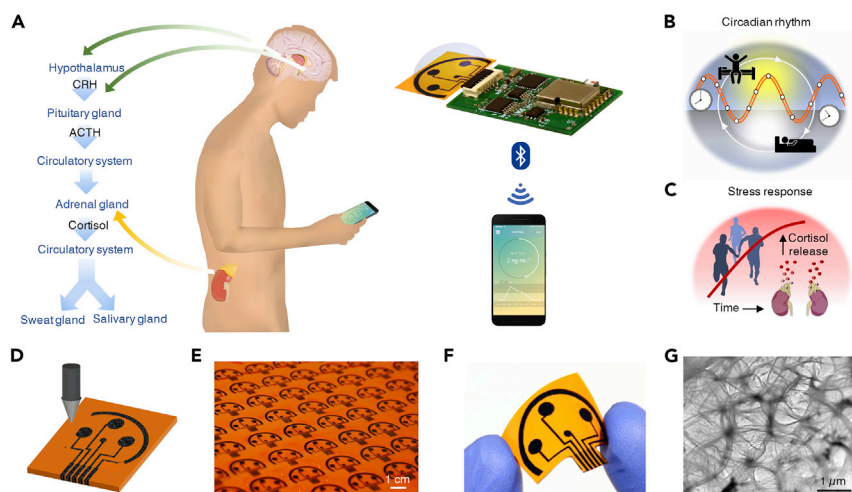


**Figure 1. An Integrated Wireless Graphene-Based Sweat Stress Sensing System (GS<sup>4</sup>) for Dynamic and Non-invasive Stress Hormone Analysis**

(A) Schematic illustration of the origin of cortisol in sweat and saliva and the use of the GS<sup>4</sup> to track the circulating cortisol level. CRH, corticotropin-releasing hormone; ACTH, adrenocorticotropic hormone.

(B and C) Conceptual illustration of cortisol dynamics regulated by circadian rhythm (B) and triggered by physiological and psychological stress (C).

(D) Illustration of the laser-engraving process of a graphene platform.

(E) Graphene sensor arrays mass-produced on a polyimide substrate.

(F) Image of a disposable flexible graphene sensor array.

(G) TEM image of the graphene electrode surface.

longitudinal stress-response studies; however, their inherent idiosyncrasy imposed by subjective interpretations challenges the accuracy of “stress level” assessment.<sup>6,7</sup> Quantification of stress hormones in biological fluids provides measurable physiological indicators for mental distress. For example, the disturbances in circadian patterns of a key stress hormone, cortisol, are linked to PTSD and major depressive disorder (Figure 1B).<sup>8,9</sup> In addition, the cortisol dynamics in stress response plays a crucial role in human performance (Figure 1C).<sup>10</sup> Other than the direct assessment of stress, stress hormones are also important in the understanding of pain and fear neural circuits,<sup>11,12</sup> both of which are subjective sensation or emotion that are difficult to quantify. Blood testing, albeit being the most well-studied hormone assessment method, is afflicted by its invasive nature and potential role as a stress stimulus. Saliva and sweat analyses, on the other hand, offer an attractive alternative for non-invasive stress hormones dynamics studies.

Recent advances in wearable and mobile health (mHealth) sensing systems have opened up a window of opportunities for hassle-free, real-time, personalized physiological data collection.<sup>13–21</sup> Substantial progress in the realm of wearable physical sensing platforms has been made with systems capable of documenting physical and kinematic data such as temperature,<sup>22</sup> pulse rate,<sup>23</sup> and ECG<sup>24</sup> in real time. Although human sweat contains rich health information and could allow non-invasive molecular monitoring, the majority of the wearable or portable systems available for sweat chemical biomarker dynamics studies are still limited to high concentration (usually at millimolar level) analytes such as pH, sodium, chloride, and glucose.<sup>25–30</sup> To date, the reported sweat hormone sensors were generally characterized in either buffer or artificial sweat samples,<sup>31,32</sup> and the dynamics of the sweat stress hormones has not yet been well studied.

<sup>1</sup>Andrew and Peggy Cherng Department of Medical Engineering, Division of Engineering and Applied Science, California Institute of Technology, Pasadena, CA 91125, USA

<sup>2</sup>Department of Psychiatry and Behavioral Neurosciences, Cedars-Sinai Medical Center, Los Angeles, CA 90048, USA

<sup>3</sup>These authors contributed equally

<sup>4</sup>Lead Contact

\*Correspondence: [weigao@caltech.edu](mailto:weigao@caltech.edu)  
<https://doi.org/10.1016/j.matt.2020.01.021>

In this work, we investigate the dynamics of the sweat stress hormone using an integrated wireless mHealth device, the graphene-based sweat stress sensing system (GS<sup>4</sup>) (Figure 1A). As a proof of concept, cortisol is selected as the model stress hormone for dynamic profiling. Highly sensitive, selective, and efficient cortisol sensing in human sweat and saliva is achieved through a unique approach that combines the laser-induced graphene and competitive immunosensing. We report here, for the first time, the cortisol diurnal cycle and the dynamic stress-response profile constructed from sweat using an integrated sensing device (Figure 1A). A strong correlation between sweat and serum cortisol levels is obtained from a small-scale pilot study. Such a wearable and point-of-care device-enabled non-invasive sweat analysis would add another dimension to stress monitoring, since it offers minimal disturbance of daily routines and could provide instantaneous and continuous assessments on subjects' psychological state.

## RESULTS AND DISCUSSION

### Design of the Graphene-Based Cortisol Sensor

The key component of our GS<sup>4</sup> platform is a flexible five-electrode graphene sensor patch fabricated on a polyimide (PI) substrate via laser engraving as illustrated in Figures 1D–1F. It boasts the advantage of rapid, scalable, and low-cost production (Figure 1E), and does not require elaborate lithography equipment or fabrication masks as compared with screen-printed electrodes. The flexible sensor patch consists of three graphene working electrodes (WEs), one Ag/AgCl reference electrode (RE), and one graphene counter electrode (CE) as depicted in Figure 1F. Detection of cortisol in human sweat is achieved through the combination of carboxylate-rich pyrrole-derivative grafting and subsequent modification on graphene surface, and a competitive sensing strategy. The large surface area and fast electron mobility of graphene offers superior performance in electrochemical sensing (Figure 1G),<sup>33</sup> while competitive immunosensing strategies offer major advances in highly selective small hormone molecule detection.<sup>34</sup>

### Electrochemical Characterization and Validation of the Cortisol Sensor

Figure 2A illustrates the process of sweat analysis and the sequential surface modification of graphene electrodes for cortisol determination, respectively. In the event of sweat analysis, sweat cortisol and horseradish peroxidase (HRP)-labeled cortisol compete for binding onto antibody-modified graphene electrode surface; enzymatic reduction of hydrogen peroxide mediated by hydroquinone generates a cathodic current that is inversely proportional to the amount of cortisol in biofluids. The detailed surface-modification procedure of graphene electrodes is schematized in Figures 2B and S1. Polymerization of 1H-pyrrole propionic acid (PPA) improves the strength and adhesion of polymeric films to transducer surfaces and facilitates subsequent surface modifications with carboxylate moieties for affinity-based sensor fabrication. In contrast to conventional graphene modification techniques such as acid reflux or monolayer formation of aryl hydrocarbon derivative, the electro-grafting of pyrrole derivative is fast (~260 s), controlled, and scalable (by connecting electrodes in parallel). Upon electropolymerization of PPA, the graphene electrode is activated by 1-ethyl-3-(3-dimethylaminopropyl)carbodiimide (EDC) and *N*-hydroxysulfosuccinimide (Sulfo-NHS) for covalent immobilization of anti-cortisol monoclonal antibody, followed by deactivation of unreacted sites with bovine serum albumin (BSA). This surface biomodification is universal to all bioaffinity receptor immobilization and could be adapted for other hormone antibodies. After brief incubation of the sensor with sweat containing the enzymatic tracer (HRP-labeled cortisol), amperometric response at  $-0.2$  V (versus Ag/AgCl) in the presence of detection substrate (hydroquinone/H<sub>2</sub>O<sub>2</sub>) is recorded.

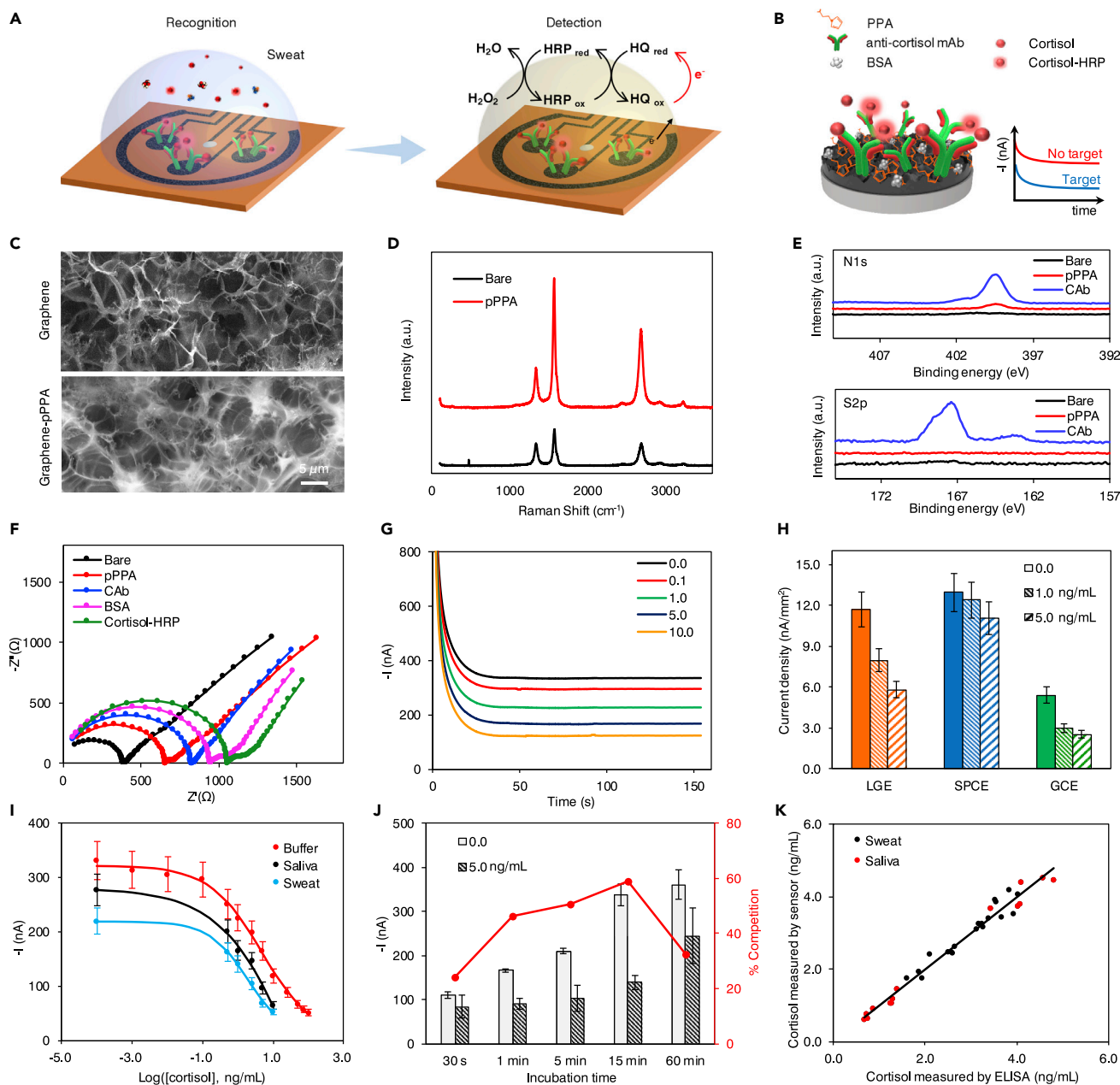


**Figure 2. Characterization and Validation of the Electrochemical Sensor for Non-invasive Cortisol Analyses**

(A and B) Schematic of the electrochemical detection of cortisol in human sweat (A) and representation of the affinity-based electrochemical cortisol sensor construction and sensing strategy (B). HRP, horseradish peroxidase; HQ, hydroquinone; PPA, pyrrole propionic acid; BSA, bovine serum albumin; mAb, monoclonal antibody.

(C) SEM images of the graphene electrode surface before and after PPA polymerization.

(D and E) Raman spectra (D) and X-ray photoelectron spectra (E) of bare graphene electrode, and graphene electrodes modified with PPA (pPPA) and capture antibody (CAB).

(F) Nyquist plots of a graphene electrode in a 0.01 M PBS solution containing 2.0 mM K<sub>4</sub>Fe(CN)<sub>6</sub>/K<sub>3</sub>Fe(CN)<sub>6</sub> (1:1) after each surface-modification step: bare graphene, electropolymerization of PPA (pPPA), capture antibody immobilization (CAB), blocking with BSA, and incubation with enzyme-tagged cortisol (cortisol-HRP).

(G) Amperometric signals of the flexible graphene-based biosensors for 0.0–10.0 ng/mL cortisol in 0.01 M PBST (pH 7.4).

(H) Sensor performance of laser-induced graphene electrode (LGE), screen-printed carbon electrode (SPCE) and glassy carbon electrodes (GCE). Current densities were obtained from 0.0, 1.0, and 5.0 ng/mL cortisol solutions. Data are presented as mean ± standard deviation (SD) (n = 3).

(I) Full sigmoidal calibration curves constructed for cortisol in buffer, sweat, and saliva. The sweat and saliva samples were collected from a healthy subject. Data are presented as mean ± SD (n = 3).

**Figure 2. Continued**

(J) Amperometric responses and percentage competition observed for 0.0 and 5.0 ng/mL cortisol with 30-s, 1-min, 5-min, 15-min, and 60-min incubation. Data are presented as mean  $\pm$  SD ( $n = 3$ ).

(K) Validation of the flexible graphene-based biosensors toward cortisol monitoring in real samples with ELISA.

To confirm the successful sensor modification, we characterized material properties of the graphene surface by scanning electron microscopy (SEM), Raman spectroscopy, and X-ray photoelectron spectroscopy (XPS) (Figures 2C–2E). The decrease in  $I_D/I_G$  value in the Raman spectrum after surface modification implies the improvement of defect concentration after a thin uniform layer of pyrrole derivative is deposited (Figure 2D). The significantly increased N1s and S2p peaks in XPS (Figure 2E) indicate the successful activation of the surface and the immobilization of the capture antibody on the sensing electrode. Moreover, open circuit potential-electrochemical impedance spectroscopy (OCP-EIS) and differential pulse voltammetry (DPV) techniques were applied to electrochemically characterize the surface after each modification step involved in the affinity-based assay. Nyquist plots for the graphene electrode exhibit increasing resistance after each modification step as a consequence of impeded interfacial electron transfer between the redox probe in solution and the functionalized transducer surface (Figure 2F). The successful polymer deposition and the effective affinity bioreceptor immobilization on the modified graphene surface were also confirmed by DPV (Figure S2). The effect of HRP-labeled cortisol concentration on amperometric responses was investigated. A dilution factor of 200 was chosen, as it yields the largest ratio between currents for 0.0 ng/mL ( $I_{0,0}$ ) and 10.0 ng/mL ( $I_{10,0}$ ) cortisol (Figure S3).

The performance of the as-prepared sensor was evaluated by measuring amperometric readout in phosphate-buffered saline (PBS) solutions containing varied cortisol concentrations (Figure 2G). Sensors prepared with laser-induced graphene electrodes (LGEs) demonstrate a much higher sensitivity with 6- and nearly 2-fold reduction in current density between 0.0 and 1.0 ng/mL (3.72 versus 0.68 and 3.72 versus 2.41 nA/mm<sup>2</sup>) as compared with screen-printed carbon electrodes (SPCEs) and glassy carbon electrodes (GCEs), respectively (Figure 2H). Amperometric signals ( $I$ ) obtained with competitive strategies are best described by a sigmoidal curve using the four-parameter logistic model following the equation<sup>35</sup>

$$I = i_1 + \frac{i_2 - i_1}{1 + 10^{(\log(C_{50} - x) \times p)}}$$

where  $i_2$  and  $i_1$  indicate the maximum and minimum current values of the dose-response curve obtained,  $IC_{50}$  represents the level of cortisol at which the amperometric signal decreases to 50% of the maximum current,  $x$  is the cortisol concentration in log scale, and  $p$  is the Hill slope at the inflection point of the sigmoid curve. Sigmoidal calibration plots of cathodic currents as a function of cortisol concentrations in buffer, sweat, and saliva samples from a healthy subject are presented in Figure 2I. No significant slope variations are observed between data obtained in human biospecimens and in buffered solutions. The limit of detection, calculated as the concentration of cortisol that produces 10% inhibition binding of HRP-labeled tracer to the immobilized affinity receptor (i.e., 10% signal reduction), is 0.08 ng/mL. The concentration range for 20%–80% inhibition binding of the enzymatic tracer is 0.43–50.2 ng/mL cortisol, covering the physiologically relevant range in sweat and saliva samples reported in previous studies.<sup>36–38</sup>

Considering that human sweat exhibits huge interpersonal variations in pH and salt content, the performance of the sensors under various pH levels and ionic strength conditions was evaluated (Figures S4A and S4B). The consistent sensor signals

indicate the universality of the sigmoidal calibration curve constructed. In addition, the selectivity of our cortisol sensor was investigated by comparing the sensor responses in the presence of other non-target hormones. As illustrated in Figure S4C, no cross-reactivity is observed for  $\beta$ -estradiol, progesterone, and cortisone.

Target binding is the rate-determining factor in bioaffinity sensors. To ensure rapid analysis and allow sufficient time for binding, we investigated a crucial criterion at the point of care, namely the effect of competition time on sensor responses. Figure 2J shows the amperometric responses obtained for 0.0 and 5.0 ng/mL cortisol with different incubation times (30 s, 1 min, 5 min, 15 min, and 60 min). The 15-min recognition time is employed for real sample analysis presented in this work in order to ensure accurate quantitation of ultra-low levels of cortisol in biofluids with a high contrast-to-noise ratio. Here, the incubation time selected is based on the experimental observation of the optimum competition rate rather than the time for binding equilibrium, as the equilibrium time is long for a heterogeneous system. Nonetheless, significant competition (47%) is observed for 5.0 ng/mL cortisol with even 1-min incubation, indicating that our sensor is capable of being close to real-time analysis of sweat cortisol at the ng/mL level (much faster compared with recent published sensing methodologies).<sup>31,38</sup> One potential strategy to further shorten the incubation time is through enhanced mixing to promote the availability of unbound cortisol to antibodies on the graphene surface.

Endogenous circulating cortisol levels in human body fluids measured with the proposed methodology in human sweat samples (as well as saliva samples, collected from eight healthy participants) were validated with the gold-standard enzyme-linked immunosorbent assay (ELISA). A high correlation between the results from the ELISA and the sensors ( $r = 0.973$ ) was obtained (Figure 2K), endorsing the accuracy of rapid cortisol quantification with our device. In addition, the sensors retained good amperometric responses (>90%) after storing at 4°C for 7 days (Figure S5).

### Systems Integration and Validation toward Personalized Sweat Sampling and Analysis

In the GS<sup>4</sup>, a three-working-electrode (3WE) sensor array design with a Ag/AgCl RE and a graphene CE that provides simultaneous multichannel readings is employed. The multichannel design provides additional accuracy via signal averaging and can potentially be adapted as a hormone panel sensor for multiplexed detection of stress-related hormones. To minimize the variation of current readout due to the ohmic drop in a non-ideal electrochemical cell (Figure S6), we position the RE and CE in equidistance from each working electrode with a suitable geometric design as shown in Figure 3A. A microfluidic module is integrated into the flexible graphene sensor patch to enable the on-body sweat sampling and *in situ* cortisol recognition (Figure 3A). This design minimizes the errors caused from the sweat evaporation and skin contamination from the traditional sweat collection, leading to nearly real-time stress hormone monitoring. Figure 3B illustrates block diagrams of functional units of the integrated electronic system that takes amperometric measurements from three channels concurrently, and wirelessly transmits the acquired data to a user device over Bluetooth Low Energy. The compact device, including a 3.7-V lithium-ion polymer battery mounted underneath a printed circuit board (PCB), is 20 × 35 × 7.3 mm in dimension. Fully functioning GS<sup>4</sup> drew 13.3 mA per second from a 150-mAh 3.7-V battery during an amperometric measurement, enabling 330 min of continuous amperometric measurements. The operation time can be significantly improved by incorporating the sleeping mode for the microcontroller and Bluetooth modules.

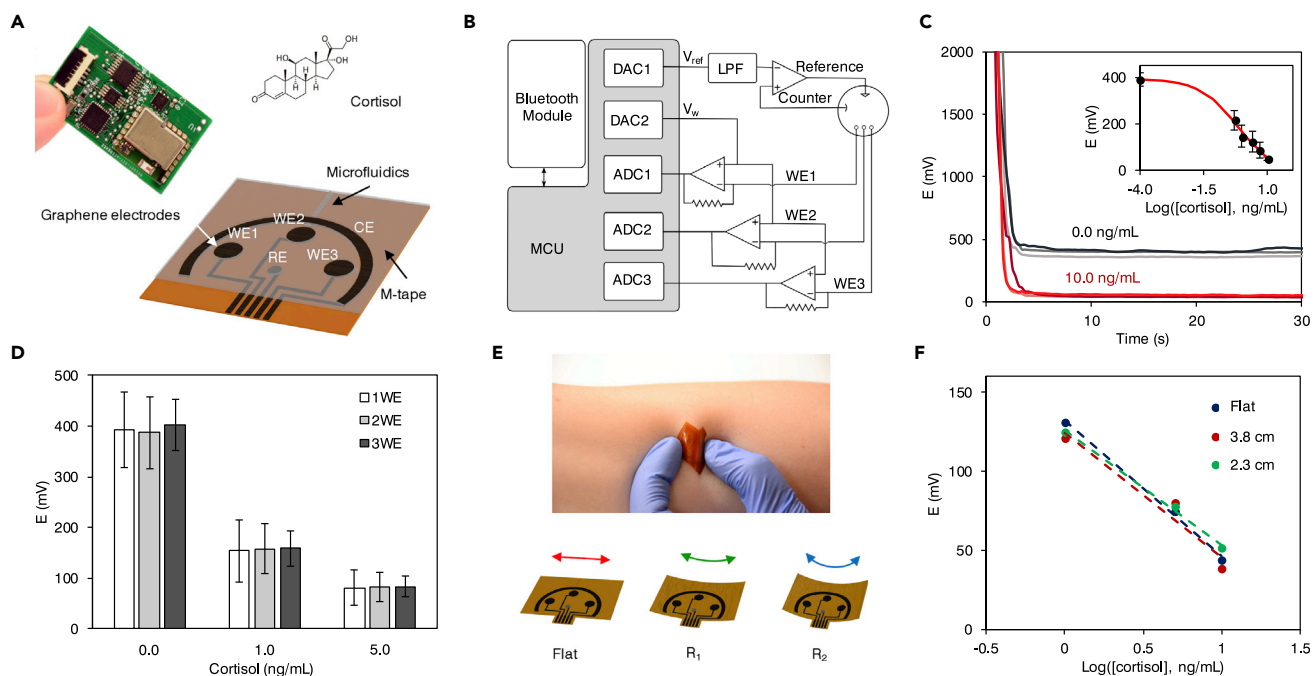


**Figure 3. System Integration and Validation of the GS<sup>4</sup> toward Personalized On-Body Use**

(A) Design of the flexible microfluidic three-working-electrode (3WE) sensor array for cortisol detection and photograph of the printed circuit board with the graphene sensor patch for signal processing and wireless communication. WE, working electrode; CE, counter electrode; RE, reference electrode. (B) Block diagram of the GS<sup>4</sup>. MCU, microcontroller unit; LPF, low-pass filter; DAC, digital-to-analog converter; ADC, analog-to-digital converter. (C) Sensor readings obtained wirelessly with the GS<sup>4</sup>. Data from inset are presented as mean  $\pm$  SD ( $n = 3$ ). (D) Comparison of average signals and SDs obtained with 1, 2, and 3 working electrodes. Data are presented as mean  $\pm$  SD ( $n = 8$ ). (E) The flexible microfluidic graphene sensor array on the skin and under mechanical deformation. (F) The responses of the sensor arrays with cortisol recognition under mechanical deformation (with radii of bending curvatures of 2.3 and 3.8 cm in 1.0, 5.0, and 10.0 ng/mL cortisol).

Representative three-channel amperometric responses obtained with the GS<sup>4</sup> are shown in Figure 3C. The calibration plot was constructed from the potential difference obtained with the GS<sup>4</sup> in the buffer solutions with five concentrations of cortisol in the pseudolinear region of the full sigmoidal plot (Figure 3C, inset). It should be noted that stable wireless sensor readings can be achieved within 10 s of measurement, indicating the rapid sensing capability of the GS<sup>4</sup>. To validate that three-channel averaging indeed provides more precise reading, we collected current readouts for 0.0, 1.0, and 5.0 ng/mL cortisol solutions, respectively from eight different sensors, followed by enumerations of all two-element and three-element combinations of the datasets and random selection of eight combinations in MATLAB to simulate two- and three-channel readings obtained with a sensor array. Error bars representing standard deviations of the simulated 2WE and 3WE readings demonstrate that the adoption of a 3WE system reduces inter-assay variation, as shown in Figure 3D. Recovery study performed on a real human sweat sample spiked with 0.0, 1.0, 2.5, and 5.0 ng/mL cortisol using the GS<sup>4</sup> shows an average 94.2% recovery (Figure S7), suggesting a low systematic error.

The flexible, disposable microfluidic sensor patch shows excellent mechanical flexibility and can conformally laminate on the skin (Figure 3E). As a demonstration of the influence of the mechanical deformation during the on-body recognition on the cortisol determination, responses of the flexible graphene sensor patch in 1.0, 5.0, and 10.0 ng/mL cortisol solutions incubated under different bending curvatures



were recorded, illustrated in [Figure 3F](#). No apparent variations in the sensor read-outs are observed with or without deformation, indicating high mechanical and electrochemical stability regarding on-body use. Considering that the actual temperature of the sensor patch during sweat collection could be significantly higher than the room temperature ([Figure S8](#)), a temperature-effect study was performed to evaluate the performance of the GS<sup>4</sup>. The sensors present no significant variation in the signals obtained for 0.0, 1.0, and 5.0 ng/mL cortisol under various temperatures (25°C, 31°C, and 37°C) ([Figure S9](#)).

Compared with the current standard analytical methods for hormone analysis such as ELISA, the GS<sup>4</sup> has distinct capabilities in multiplexed monitoring, miniaturization, a short assay time (down to 1 min versus 80 min), and a smaller required sample volume (<10  $\mu$ L versus 100  $\mu$ L), making it an ideal platform for subsequent investigations on dynamic sweat cortisol variations and potential applications in personalized health management.

### Investigation of the Circadian Rhythm of Sweat Cortisol

Cortisol presents a distinct and robust diurnal pattern, which peaks shortly after awakening and declines throughout the day in plasma<sup>39</sup> and saliva.<sup>40,41</sup> Early reports showed that sweat contains cortisol levels comparable with those reported in saliva;<sup>42</sup> we postulate that circulating cortisol molecules are transported to and stored in eccrine and apocrine glands, secreted into the sweat, and ultimately excreted through a sweat pore to the epidermal surface.<sup>43</sup> It is, therefore, reasonable to hypothesize that cortisol level in sweat might present similar circadian rhythm regulated by the internal clock and light/dark cycle ([Figure 4A](#)). Considering that the circadian pattern of circulating cortisol is highly informative for a number of mental health conditions,<sup>8,9</sup> the fluctuations of the ultra-low levels of sweat cortisol were investigated with the graphene platform through a pilot human study. Sweat was sampled with iontophoretic sweat stimulation as illustrated in [Figure S10](#).

[Figure 4B](#) illustrates the reproducible patterns obtained from an exploratory study by monitoring the sweat cortisol variations of a healthy subject in a period of 6 days. High morning (AM) cortisol level and low afternoon (PM) level are observed each day; such rhythm resembles diurnal cycles of circulating cortisol in blood. To further characterize the correlation between sweat and circulating cortisol levels, we analyzed sweat in the early AM and the late PM from four healthy subjects along with saliva and serum. A similar trend in AM/PM cortisol variations modulated by circadian rhythm are observed from all samples ([Figures 4C–4F](#)), with the ratios ranging from 1.35 to 2.00. Although several studies explored the correlation of cortisol found in various biofluids including blood, urine, and saliva,<sup>44–46</sup> the relationship between sweat and circulating cortisol levels, to the best of our knowledge, has barely been explored. A positive correlation between sweat cortisol and serum cortisol (Pearson's correlation coefficient  $r = 0.87$ ) ([Figure 4G](#)) was obtained based on data collected from eight healthy subjects. Similarly, the correlation coefficient between sweat cortisol and salivary cortisol was determined to be 0.78 ([Figure 4H](#)). Although the number of real samples analyzed is limited in this exploratory study, empirical evidence suggests that a strong correlation exists between sweat cortisol and serum cortisol.

### Dynamic Cortisol Response to Stress Stimuli

In addition to long-term profiling of the diurnal cycles, cortisol response to acute stressors contains abundant information for psychoneurological investigations,<sup>47,48</sup> and plays a critical role in human performance monitoring and management.<sup>1</sup> For

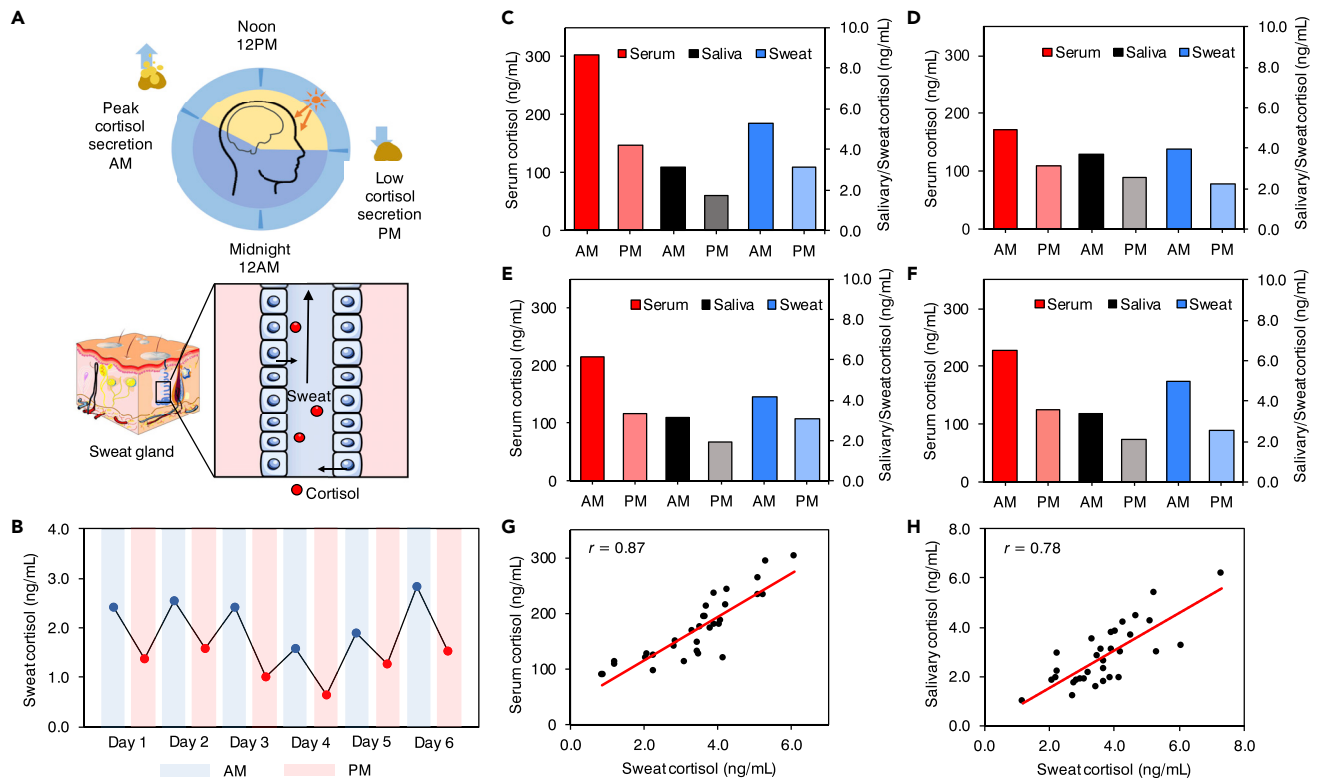


**Figure 4. Investigation of the Circadian Rhythm of Sweat Stress Hormone Using the GS<sup>4</sup>**

(A) Conceptual illustration of the light/dark-cycle-regulated cortisol circadian rhythm and the transport of circulating cortisol to sweat.

(B) Circadian rhythm of sweat cortisol constructed for a healthy subject in a period of 6 days. Sweat was sampled and analyzed in the morning (AM) and afternoon (PM) each day.

(C–F) Cortisol levels found in serum, saliva, and sweat sampled in the AM and PM from four healthy subjects.

(G) Correlation of serum cortisol with sweat cortisol. The correlation coefficient  $r$  was acquired through Pearson's correlation analysis (eight subjects,  $n = 4$  for each subject,  $p < 0.001$ ).

(H) Correlation of salivary cortisol with sweat cortisol. The correlation coefficient  $r$  was acquired through Pearson's correlation analysis (eight subjects,  $n = 4$  for each subject,  $p < 0.001$ ).

instance, sensitization of the HPA axis to external stimuli is another critical factor that distinguishes PTSD from other psychiatric disorders.<sup>8</sup> Next, we set out to investigate whether sweat analysis of cortisol presents meaningful changes to acute stress of the human subjects induced by different stressors in a short time frame.

Aerobic exercises such as running and cycling are potent stimuli/stressors of cortisol secretion.<sup>49</sup> In this study, a 50-min stationary cycling exercise at a constant workload was employed for sweat cortisol content analysis (Figure 5A). Sweat sampling and analysis were performed with the GS<sup>4</sup> sequentially at 10-min intervals for the 50-min constant-load exercise in a cycling ergometer from three physically untrained subjects and one trained (athletic) subject. In addition, serum cortisol levels before and immediately after the cycling exercise were analyzed to validate whether sweat cortisol variation is in accordance with circulating cortisol levels. For all subjects under study, sweat cortisol increases progressively and reaches the highest level after 40 min of continuous biking. From this point, a slight decrease in cortisol level is detected near the end of the exercise in all participants and more significantly in subject 4 (athlete) (Figure 5B). Cortisol contents in pre- and post-exercise serum samples present a good correlation with the change in cortisol from the beginning of perspiration (10 min) to the end of the exercise (50 min) (Figure 5C). The dynamic sweat

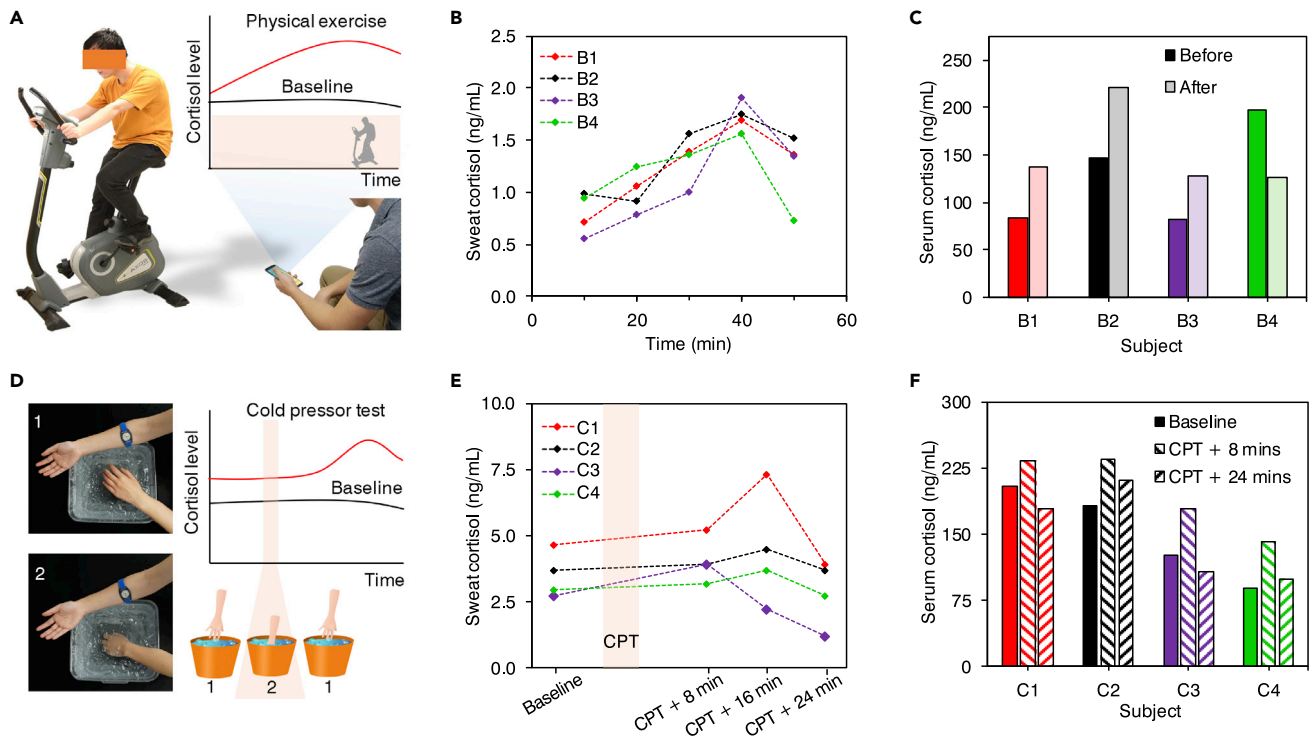


**Figure 5. Dynamic Monitoring of Stress Response Using GS<sup>4</sup>**

- (A) Conceptual illustration of stress-response monitoring by tracking of a subject's cortisol level with data wirelessly transmitted to a cellphone via Bluetooth. Physical exercise is utilized as a stressor.
- (B) Cortisol monitoring from three physically untrained subjects (B1–B3) and one trained subject (B4) in a constant-load cycling exercise.
- (C) Cortisol levels in serum sampled and analyzed before and after the cycling exercise for four subjects.
- (D) Illustration of stress response in relation to the time frame of cold pressor test (CPT) performance.
- (E) Cortisol monitoring from four subjects (C1–C4) undergoing the CPT. Dynamic cortisol response was evaluated with iontophoresis sweat from the forearm sampled and analyzed at 10-min intervals.
- (F) Cortisol levels in serum sampled before, 8 min after, and at the end of the CPT experiment.

hormone profiles observed for untrained subjects are similar to reported trends of serum cortisol after high-intensity exercise,<sup>50</sup> indicating the activation of HPA by physical exercise. In contrast, the blunted cortisol response observed in the trained subject reflects exercise-induced adaptation. This is consistent with previous reports that trained individuals likely perceive the given workload as a smaller stressor and demonstrate a lower degree of HPA activation in response to physical stressors<sup>51</sup> as well as psychosocial stimuli.<sup>52</sup>

Noting that circadian patterns in sweat cortisol level give rise to different baselines before stress stimulation, cortisol variations in sweat for physical exercises conducted in the morning and in the afternoon for the same subjects were studied. Sweat cortisol levels were analyzed from two subjects at the beginning of the perspiration and at the end of the cycling (Figure S11). Significantly increased sweat cortisol levels are observed at 50 min as compared with that at 10 min, in response to the physiological stressor. Cortisol level for the first time point is higher in the AM than in the PM for both subjects; higher relative percentage change of cortisol is observed in the PM exercise. This relation is in agreement with the diurnal sweat cortisol variation we observed in the circadian rhythm study, similar to a previous report that shows the circadian rhythm of serum and salivary cortisol could confound the magnitude of cortisol responses.<sup>53</sup> These results reveal the importance of baseline construction

in offsetting circadian baseline in the context of short-term dynamic sweat cortisol stress response. Point-of-care and wearable devices-enabled sweat analysis could conveniently facilitate personalized baseline construction as discussed for the circadian rhythm study.

To study the response time frame of sweat cortisol to acute stressors, we performed an exploratory cold pressor test (CPT) on four subjects. Subjects were asked to immerse their non-dominant hand in iced water for 3 min (Figure 5D). CPT is a reliable acute physiological stressor that triggers immediate HPA-axis activation and significant cortisol release.<sup>54</sup> Sweat was sampled at 8-min intervals with iontophoretic sweat stimulation as illustrated in Figure S10. The sweat dynamic cortisol profile was evaluated in each case. We observed that cortisol increased after completion of CPT, reaching the mean peak between 8 and 16 min after CPT (Figure 5E). Similar trends were also observed for serum (Figure 5F) and salivary cortisol (Figure S12); the former was collected and tested before starting the experiment (denoted as baseline) and at 8 and 24 min after CPT. These observations are consistent with previously reported CPT studies for evaluation of release of cortisol and other hormones in serum<sup>55</sup> and saliva.<sup>56</sup> The sweat cortisol profiles presented small to negligible time lag compared with serum cortisol trends in the literature,<sup>57–59</sup> revealing the promptness of sweat cortisol as a quasi-real-time stress indicator. Furthermore, given the clinical applicability of CPT for evaluation of pain tolerance,<sup>60</sup> sweat stress hormones sensors may serve as an attractive quantification approach in pain perception studies.

### Conclusion

This work demonstrates the potential of sweat hormone analysis enabled by an integrated portable system, the GS<sup>4</sup>. Highly sensitive, selective, and efficient stress hormone sensing was achieved through a unique combination of the laser-induced graphene and immunosensing. The assay time could be as low as 1 min. Using this graphene-based wireless sensing platform, we have demonstrated that relevant information crucial to stress response and adaptation analysis could be extracted from cortisol excreted in sweat. The low-cost and mass-produced graphene sensor arrays enabled us to conduct several meaningful stress-related physiological studies. To the best of our knowledge, the results we present here represent the first demonstration of the cortisol diurnal cycle and the dynamic stress-response profile constructed from human sweat. On a longer time scale, characteristic cortisol circadian rhythms could be monitored; in a short time frame, acute external stimuli-triggered stress response could be analyzed.

This study unveils the immense potential of sweat cortisol circadian variation monitoring. Sweat's accessibility to wearable continuous monitoring devices and its minimal invasiveness enables the construction of long-term and comprehensive cortisol diurnal patterns. To date, many clinical studies on psychological disorder-triggered cortisol circadian rhythm variation rely heavily on data collected at sparsely spaced plasma or saliva cortisol sampling timing,<sup>61,62</sup> whereas those with narrow sampling intervals were achieved with intravenous catheters;<sup>63</sup> confirmation of cortisol circadian rhythms in sweat might revolutionize clinical research and mental health monitoring paradigms for both clinicians and patients in the near future.

The possibility of continuous dynamic stress-response profiling with sweat sensors offers new opportunities for fundamental psychoneuroendocrinology studies and timely documentation of stress levels for day-to-day mental health monitoring. Although only physical stress stimuli were investigated in the present study, given

the fact that psychosocial stress stimuli trigger similar neuroendocrine and behavioral responses regulated by the HPA axis,<sup>3</sup> similar information may be extracted from sweat cortisol in response to psychosocial stresses. The good correlation with circulating hormones, the diurnal cycle, and the dynamic stress-response profile demonstrated in this study using our integrated sensing approach will lead the next wave of technological advancement in personalized human performance and mental health management.

## EXPERIMENTAL PROCEDURES

### Materials and Reagents

PPA (97%), EDC, Sulfo-NHS, BSA, hydroquinone, 2-(*N*-morpholino)ethanesulfonic acid (MES), Tween 20, hydrocortisone, cortisone, progesterone,  $\beta$ -estradiol, sodium thiosulfate, sodium bisulfite, and potassium ferrocyanide(II) were purchased from Sigma-Aldrich. Sodium dihydrogen phosphate, potassium hydrogen phosphate, potassium chloride, hydrogen peroxide (30% (w/v)), and sulfuric acid were purchased from Fisher Scientific. Potassium ferricyanide(III) and silver nitrate, and iron(III) chloride and 0.1 M PBS (pH 7.4) were purchased from Acros Organics and Alfa Aesar, respectively. Anti-cortisol murine monoclonal antibody and HRP-labeled cortisol were purchased from EastCoastBio. A cortisol-competitive human ELISA kit (catalog no. EIAHCOR) was purchased from Thermo Fisher. PI film (75  $\mu$ m thick) was purchased from DuPont.

### Fabrication of Three-Channel Array Electrode

For three-channel graphene sensor fabrication, a PI film was attached onto a supporting substrate in a 50-W CO<sub>2</sub> laser cutter (Universal Laser System). Selected laser-cutting parameters were: power 5.0%, speed 6%, points per inch 1,000, in raster mode and at focused height. Ag/AgCl REs were fabricated by electrodeposition in 20  $\mu$ L of a mixture solution containing silver nitrate, sodium thiosulfate, and sodium bisulfite (final concentrations 250 mM, 750 mM, and 500 mM, respectively) for 100 s at  $-0.2$  mA, followed by drop-casting a 10  $\mu$ L-aliquot of FeCl<sub>3</sub> for 1 min.

### Modification of Sensing Platform and Electrochemical Detection

PPA electropolymerization was conducted by cyclic voltammetry (CV) from 0.0 to 0.85 V (versus Ag/AgCl) for 20 cycles at a scan rate of 0.1 V/s in a fresh solution containing 5.0 mM carboxyl-functionalized pyrrole monomer and 0.5 M KCl. After rinsing with deionized water and drying under air flow, electrodes were incubated with 10  $\mu$ L of a mixture solution containing 0.4 M EDC and 0.1 M Sulfo-NHS in 0.025 M MES (pH 5.0) for 35 min at room temperature under humid ambient conditions. Covalent attachment of specific antibody onto activated surface was carried out by drop-casting 10  $\mu$ L of anti-cortisol antibody solution (100  $\mu$ g/mL in MES buffer (pH 5.0)) and incubated at room temperature for 90 min, followed by a 1-h blocking step with 1.0% BSA prepared in 0.01 M phosphate-buffered saline with Tween 20 (PBST) at pH 7.4. After one washing step with the same buffered solution, 10- $\mu$ L aliquots of cortisol standards (or the biofluid to be analyzed properly diluted) and HRP-cortisol (1/200 dilution) prepared in PBST (pH 7.4) were drop-cast onto the working electrode, allowing competition between labeled and circulating free cortisol contained in the sample for the available free sites of the immobilized affinity receptor to take place for 15 min. Amperometric readings were registered at  $-0.2$  V (versus Ag/AgCl) in 50 mM sodium phosphate buffer (pH 6.0) containing 2.0 mM hydroquinone. The readout signal was obtained after a 30- $\mu$ L aliquot of 10 mM H<sub>2</sub>O<sub>2</sub> was injected to the system.

### Characterization of the Biosensing Platform

The morphology and material properties of the graphene sensing electrodes before and after surface modification were characterized by transmission electron microscopy (TEM), SEM, Raman spectroscopy, and XPS. The SEM images of graphene electrodes were obtained by a focused ion-beam scanning electron microscope (FEI Nova 600; NanoLab). TEM images were obtained by a transmission electron microscope (Tecnai TF-20). The surface properties of the laser-induced graphene were characterized by an X-ray photoelectron spectroscope (Escalab 250xi; Thermo Scientific). Raman spectrum of the graphene was recorded using a 532.8-nm laser with an inVia Reflex confocal laser microscope (Renishaw, UK).

Amperometry, OCP-EIS, CV, and DPV were carried out on a CHI820 electrochemical station by means of an electrochemical setup comprising LGEs as the WEs, a platinum wire as the CE, and a commercial Ag/AgCl electrode as the RE.

To characterize surface modification after each step electrochemically, we carried out DPV and OCP-EIS readings in 0.01 M PBS (pH 7.4) containing 2.0 mM  $K_4Fe(CN)_6/K_3Fe(CN)_6$  (1:1) at detailed conditions: potential range,  $-0.3$  and  $0.6$  V; pulse width, 0.2 s; incremental potential, 4 mV; amplitude, 50 mV; frequency range,  $0.1$ – $10^6$  Hz; amplitude, 5 mV. Performances of LGEs, GCEs, and commercial SPCEs were compared through current densities ( $nA/mm^2$ ) obtained after developing the proposed competitive-based assay on both carbon surfaces for target cortisol determination at 1.0- and 5.0-ng/mL levels under optimized conditions. Dilution of HRP-labeled cortisol was optimized by comparing amperometric responses obtained for 1/100, 1/200, and 1/300 diluted enzymatic tracer for 0.0 and 10.0 ng/mL cortisol standards. Performance of our device was evaluated for different pHs and salt contents ranging from pH 7.4 to 4.1 and from 0.1 M to 0.001 M PBST, respectively. Selectivity test was conducted in the presence of mixture solutions of 1/200 HRP-cortisol enzymatic tracer containing 5.0 ng/mL cortisone, progesterone, or  $\beta$ -estradiol, in the absence or presence of target hormone at the same concentration level. A stability study was conducted for target cortisol determination at 5.0-ng/mL levels under optimized conditions. The electrodes for the stability study were modified on the same day and stored at  $4^\circ C$  for 0–35 days before the competitive assay was carried out.

### System-Level Development and Evaluation

The electronic system for the integrated three-channel electrochemical analyzer was designed to be compact and efficient. A two-layer PCB ( $20 \times 35 \times 0.6$  mm) had all the components on the top layer such that a 150-mAh 3.7-V lithium-ion polymer battery ( $19.75 \times 26 \times 3.8$  mm) could sit comfortably underneath the PCB. The entire device is  $20 \times 35 \times 7.3$  mm, comparable with a USB thumb drive.

The small size, low power consumption, and rich analog peripherals of the STM32L432 ultra-low-power Arm Cortex-M4 32-bit microcontroller (MCU) enabled the compact size of the overall electronic system. The MCU had a built-in 12-bit analog-to-digital converter (ADC) and two built-in 12-bit digital-to-analog converters (DACs). When a user initiates an electrochemical measurement over Bluetooth, the built-in DACs generate a reference voltage ( $V_{ref}$ ) and a working voltage ( $V_w$ ) that set the potentials at the RE and WEs through a potentiostat interface circuit. For the three-channel amperometric measurements required for cortisol analysis, the reference voltage was stabilized further by a low-pass filter, and the three WEs were biased at  $-0.2$  V relative to the RE. The resultant currents flowing through each electrode were amplified and converted to voltage by transimpedance

amplifiers. Three channels of the MCU's ADC were utilized to acquire concurrent amperometric measurements, and the data were transmitted to a user device over Bluetooth for further analysis.

To prepare the microfluidic module, we attached a double-sided medical adhesive to a substrate and cut through it using a 50-W CO<sub>2</sub> laser cutter (Universal Laser System) to make the channels and reservoir. Influence of mechanical deformation was investigated through incubating the sensor patch in the cortisol solutions for 15 min under mechanical deformation (with radii of bending curvature 2.3 and 3.8 cm).

### Subjects and Procedures

The performance of the GS<sup>4</sup> was evaluated in human sweat, saliva, and sweat samples from the human subjects in compliance with the protocols that were approved by the Institutional Review Board (no. 19-0895 and no. 19-0892) at the California Institute of Technology (Caltech). The participating subjects (12 healthy subjects, age range 18–65 years) were recruited from Caltech campus and the neighboring communities through advertisement by posted notices, word of mouth, and email distribution. All subjects gave written informed consent before participation in the study.

### Circadian Rhythm Study

Four healthy subjects who reported regular sleep-wake rhythm and no sleep disturbances participated in this study. Subjects were informed to refrain from food intake at least 30 min before reporting to the laboratory. On the experimental day, subjects reported to the laboratory at 8:00 AM and at 7:00 PM on the same day for collection of sweat, saliva, and capillary blood. Sweat stimulation was performed with a Model 3700 Macroduct by placing two electrodes on the precleaned forearm region of the subject. After their connection to the source, a 1.5-mA current was applied for 5 min, and secreted sweat was sampled for a period of 40 min and then analyzed. During the sweat sampling and test, fresh capillary blood and saliva were collected from the subject immediately after sweat stimulation following the protocol described below in the sample-processing section.

### Physiological Stress Response: Stationary Biking Study

Three untrained participants and one trained participant were involved in this study. The trained subject (an athlete from Caltech sport teams) exercised regularly for at least 9 h per week while the untrained subjects had an average of 1 h of exercise per week. Constant workload physical activity trials were performed in the morning (from 8:00 to 10:00 AM) or afternoon (from 5:00 to 7:00 PM) on an ergometer stationary bike (Kettler Axos Cycle M-LA). Subjects were informed to refrain from food intake at least 30 min before the exercise. Subjects were asked to bike for 50 min at a constant speed of 60 rpm, and sweat samples were collected every 10 min from the forehead. Before starting the aerobic trial, and after sweat sampling and analysis at each time interval, participants' foreheads were cleaned with alcohol swabs and gauze. Blood collections were performed before the stationary bike exercise and immediately after the exercise following the procedures described below in the sample-processing section.

### Physiological Stress Response: Cold Pressor Test

Four participants were exposed to standard CPT in the afternoon (between 5:00 and 7:00 PM) in order to control for the diurnal cortisol cycle. The procedure was initiated by collecting sweat through iontophoresis for a period of 8 min. At the same time,

saliva and capillary blood samples from each participant were collected with the purpose of determining baseline values. Subsequently, recruited volunteers immersed their non-dominant hand up to the wrist in a plastic tank containing cold water (2°C) for 3 min (CPT) and after the immersion time were instructed to remove the hand from the iced water. Sweat, saliva, and capillary blood were collected following the detailed protocols at different resting periods after the CPT test (8, 16, and 24 min).

### Saliva and Blood Sample Processing Protocol

After rinsing their mouth with water, volunteers deposited saliva in 1.5-mL Eppendorf tubes, which were subsequently centrifuged (10,000 rpm, 10 min) and analyzed. Fresh capillary blood samples were collected at the same periods of time as saliva using a finger-prick approach. After cleaning the fingertip with an alcohol wipe and allowing it to air dry, the skin was punctured with a CareTouch lancing device. Samples were collected in 1.5-mL Eppendorf tubes after wiping off the first drop of blood with gauze. Once the standardized clotting procedure finished, serum was separated by centrifuging at 3,575 rpm for 15 min and instantly stored at –20°C.

### ELISA for Validation of Human Sample Analysis

ELISA tests for cortisol were performed in an accuSkan FC Filter-Based Microplate Photometer at a detection wavelength of 450 nm according to the manufacturer's instructions. In brief, standards (or properly diluted samples), HRP-cortisol conjugate, and cortisol antibody were added to immunoglobulin G-coated microtiter plate wells and incubated for 1 h at room temperature. After four washing steps with wash buffer, 100  $\mu$ L of 3,3',5,5'-tetramethylbenzidine substrate was incubated for 30 min, and absorbance values were measured immediately after addition of 50  $\mu$ L of 1 M H<sub>2</sub>SO<sub>4</sub> in each well.

### Thermal Imaging of Device and Skin Temperature

Thermal images of the sensor patch on human skin were taken by a long-wave infrared thermal camera (FLIR A655sc).

### DATA AND CODE AVAILABILITY

The data that support the plots within this paper and other findings of this study are available from the corresponding author upon reasonable request.

### ACKNOWLEDGMENTS

This project was supported by the Rothenberg Innovation Initiative (RI<sup>2</sup>) program, the Carver Mead New Adventures Fund, Caltech-City of Hope Biomedical Research Initiative, and National Institutes of Health (#5R21NR018271) (all to W.G.). J.T. was supported by the National Science Scholarship from the Agency for Science, Technology and Research (A\*STAR), Singapore. We gratefully acknowledge critical support and infrastructure provided for this work by the Kavli Nanoscience Institute and Jim Hall Design and Prototyping Lab at Caltech, and we gratefully thank Dr. Matthew Hunt and Bruce Dominguez for their help. We also thank Dr. Chiara Daraio and Vincenzo Costanza for the technical support and helpful assistance with infrared imaging.

### AUTHOR CONTRIBUTIONS

W.G., R.M.T.-R., and J.T. initiated the concept; W.G., R.M.T.-R., J.T., and W.W.I. designed the experiments; R.M.T.-R. and J.T. led the experiments and collected the overall data; Y.Y. performed electrode fabrication and characterization; J.M.



performed the circuit design and test; C.X., C.Y., M.W., Y.S., and Y.Y. contributed to sensor characterization; W.G., R.M.T.-R., and J.T. contributed the data analysis and co-wrote the paper. All authors provided feedback on the manuscript.

## DECLARATION OF INTERESTS

The authors declare no competing interests.

Received: September 24, 2019

Revised: November 21, 2019

Accepted: January 27, 2020

Published: February 26, 2020

## REFERENCES

- Mariotti, A. (2015). The effects of chronic stress on health: new insights into the molecular mechanisms of brain-body communication. *Futur. Sci. OA* 1, FSO23.
- Cohen, S., Janicki-Deverts, D., and Miller, G.E. (2007). Psychological stress and disease. *J. Am. Med. Assoc.* 298, 1685–1687.
- Kogler, L., Müller, V.I., Chang, A., Eickhoff, S.B., Fox, P.T., Gur, R.C., and Derntl, B. (2015). Psychosocial versus physiological stress—meta-analyses on deactivations and activations of the neural correlates of stress reactions. *NeuroImage* 119, 235–251.
- Herman, J.P., McKlveen, J.M., Ghosal, S., Kopp, B., Wulsin, A., Makinson, R., Scheimann, J., and Myers, B. (2016). Regulation of the hypothalamic-pituitary-adrenocortical stress response. *Compr. Physiol.* 6, 603–621.
- Nicolson, N.A., and Csikszentmihalyi, M. (1992). Stress, coping and cortisol dynamics in daily life. In *The Experience of Psychopathology: Investigating Mental Disorders in Their Natural Settings*, M.W. de Vries, ed. (Cambridge University Press), pp. 219–232.
- Sladek, M.R., Doane, L.D., and Stroud, C.B. (2016). Individual and day-to-day differences in active coping predict diurnal cortisol patterns among early adolescent girls. *J. Youth Adolesc.* 46, 121–135.
- Verhagen, S.J.W., Hasmi, L., Drukker, M., Os, J.V., and Delespaul, P.A.E.G. (2016). Use of the experience sampling method in the context of clinical trials. *Evid. Based Ment. Health* 19, 86–89.
- Yehuda, R. (1997). Sensitization of the hypothalamic-pituitary-adrenal axis in posttraumatic stress disorder. *Ann. N. Y. Acad. Sci.* 821, 57–75.
- Herbert, J. (2012). Cortisol and depression: three questions for psychiatry. *Psychol. Med.* 43, 449–469.
- Bos, R.V.D., Hartevel, M., and Stoop, H. (2009). Stress and decision-making in humans: performance is related to cortisol reactivity, albeit differently in men and women. *Psychoneuroendocrinology* 34, 1449–1458.
- Rodrigues, S.M., Ledoux, J.E., and Sapolsky, R.M. (2009). The influence of stress hormones on fear circuitry. *Annu. Rev. Neurosci.* 32, 289–313.
- Uum, S.H.M.V., Sauv e, B., Fraser, L.A., Morley-Forster, P., Paul, T.L., and Koren, G. (2008). Elevated content of cortisol in hair of patients with severe chronic pain: a novel biomarker for stress. *Stress* 11, 483–488.
- Kim, J., Campbell, A.S.,  vila, B.E.-F.D., and Wang, J. (2019). Wearable biosensors for healthcare monitoring. *Nat. Biotechnol.* 37, 389–406.
- Nakata, S., Shiomi, M., Fujita, Y., Arie, T., Akita, S., and Takei, K. (2018). A wearable pH sensor with high sensitivity based on a flexible charge-coupled device. *Nat. Electron.* 1, 596–603.
- Lee, H., Choi, T.K., Lee, Y.B., Cho, H.R., Ghaffari, R., Wang, L., Choi, H.J., Chung, T.D., Lu, N., Hyeon, T., et al. (2016). A graphene-based electrochemical device with thermoresponsive microneedles for diabetes monitoring and therapy. *Nat. Nanotechnol.* 11, 566–572.
- Lee, H., Song, C., Hong, Y.S., Kim, M.S., Cho, H.R., Kang, T., Shin, K., Choi, S.H., Hyeon, T., and Kim, D.-H. (2017). Wearable/disposable sweat-based glucose monitoring device with multistage transdermal drug delivery module. *Sci. Adv.* 3, e1601314.
- Han, S., Kim, J., Won, S.M., Ma, Y., Kang, D., Xie, Z., Lee, K.-T., Chung, H.U., Banks, A., Min, S., et al. (2018). Battery-free, wireless sensors for full-body pressure and temperature mapping. *Sci. Transl. Med.* 10, eaan4950.
- Yang, Y., and Gao, W. (2019). Wearable and flexible electronics for continuous molecular monitoring. *Chem. Soc. Rev.* 48, 1465–1491.
- Bariya, M., Nyein, H.Y.Y., and Javey, A. (2018). Wearable sweat sensors. *Nat. Electron.* 1, 160–171.
- Reeder, J.T., Choi, J., Xue, Y., Gutruf, P., Hanson, J., Liu, M., Ray, T., Bandodkar, A.J., Avila, R., Xia, W., et al. (2019). Waterproof, electronics-enabled, epidermal microfluidic devices for sweat collection, biomarker analysis, and thermography in aquatic settings. *Sci. Adv.* 5, eaau6356.
- Bandodkar, A.J., Gutruf, P., Choi, J., Lee, K., Sekine, Y., Reeder, J.T., Jeang, W.J., Aranyosi, A.J., Lee, S.P., Model, J.B., et al. (2019). Battery-free, skin-interfaced microfluidic/electronic systems for simultaneous electrochemical, colorimetric, and volumetric analysis of sweat. *Sci. Adv.* 5, eaav3294.
- Zhu, C., Chortos, A., Wang, Y., Pfattner, R., Lei, T., Hinckley, A.C., Pochorovski, I., Yan, X., To, J.W.-F., Oh, J.Y., et al. (2018). Stretchable temperature-sensing circuits with strain suppression based on carbon nanotube transistors. *Nat. Electron.* 1, 183–190.
- Boutry, C.M., Beker, L., Kaizawa, Y., Vassos, C., Tran, H., Hinckley, A.C., Pfattner, R., Niu, S., Li, J., Claverie, J., et al. (2019). Biodegradable and flexible arterial-pulse sensor for the wireless monitoring of blood flow. *Nat. Biomed. Eng.* 3, 47–57.
- Son, D., Kang, J., Vardoulis, O., Kim, Y., Matsuhisa, N., Oh, J.Y., Mun, J., Katsumata, T., Liu, Y., McGuire, A.F., et al. (2018). An integrated self-healable electronic skin system fabricated via dynamic reconstruction of a nanostructured conducting network. *Nat. Nanotechnol.* 13, 1057–1065.
- Gao, W., Emaminnejad, S., Nyein, H.Y.Y., Challa, S., Chen, K., Peck, A., Fahad, H.M., Ota, H., Shiraki, H., Kiriya, D., et al. (2016). Fully integrated wearable sensor arrays for multiplexed in situ perspiration analysis. *Nature* 529, 509–514.
- Choi, J., Bandodkar, A.J., Reeder, J.T., Ray, T.R., Turnquist, A., Kim, S.B., Nyberg, N., Hourlier-Fargette, A., Model, J.B., Aranyosi, A.J., et al. (2019). Soft, skin-integrated multifunctional microfluidic systems for accurate colorimetric analysis of sweat biomarkers and temperature. *ACS Sens.* 4, 379–388.
- Heikenfeld, J., Jajack, A., Feldman, B., Granger, S.W., Gaitonde, S., Begtrup, G., and Katchman, B.A. (2019). Accessing analytes in biofluids for peripheral biochemical monitoring. *Nat. Biotechnol.* 37, 407–419.
- Kim, J., Jeerapan, I., Imani, S., Cho, T.N., Bandodkar, A.J., Cinti, S., Mercier, P.P., and Wang, J. (2016). Noninvasive alcohol monitoring using a wearable tattoo-based iontophoretic-biosensing system. *ACS Sens.* 1, 1011–1019.
- Tai, L.-C., Gao, W., Chao, M., Bariya, M., Ngo, Q.P., Shahpar, Z., Nyein, H.Y.Y., Park, H., Sun, J., Jung, J., et al. (2018). Methylxanthine drug monitoring with wearable sweat sensors. *Adv. Mater.* 30, 1707442.

30. Emaminejad, S., Gao, W., Wu, E., Davies, Z.A., Nyein, H.Y.Y., Challa, S., Ryan, S.P., Fahad, H.M., Chen, K., Shahpar, Z., et al. (2017). Autonomous sweat extraction and analysis applied to cystic fibrosis and glucose monitoring using a fully integrated wearable platform. *Proc. Natl. Acad. Sci. USA* **114**, 4625–4630.
31. Kinnamon, D., Ghanta, R., Lin, K.-C., Muthukumar, S., and Prasad, S. (2017). Portable biosensor for monitoring cortisol in low-volume perspired human sweat. *Sci. Rep.* **7**, 13312.
32. Parlak, O., Keene, S.T., Marais, A., Curto, V.F., and Salleo, A. (2018). Molecularly selective nanoporous membrane-based wearable organic electrochemical device for noninvasive cortisol sensing. *Sci. Adv.* **4**, eaar2904.
33. Shao, Y., Wang, J., Wu, H., Liu, J., Aksay, I.A., and Lin, Y. (2010). Graphene based electrochemical sensors and biosensors: a review. *Electroanalysis* **22**, 1027–1036.
34. Wang, X., Cohen, L., Wang, J., and Walt, D.R. (2018). Competitive immunoassays for the detection of small molecules using single molecule arrays. *J. Am. Chem. Soc.* **140**, 18132–18139.
35. Findlay, J.W.A., and Dillard, R.F. (2007). Appropriate calibration curve fitting in ligand binding assays. *AAPS J.* **9**, E260–E267.
36. Jia, M., Chew, W.M., Feinstein, Y., Skeath, P., and Sternberg, E.M. (2016). Quantification of cortisol in human eccrine sweat by liquid chromatography-tandem mass spectrometry. *Analyst* **141**, 2053–2060.
37. Miller, R., Plessow, F., Rauh, M., Gröschl, M., and Kirschbaum, C. (2013). Comparison of salivary cortisol as measured by different immunoassays and tandem mass spectrometry. *Psychoneuroendocrinology* **38**, 50–57.
38. Khan, M.S., Misra, S.K., Wang, Z., Daza, E., Schwartz-Duval, A.S., Kus, J.M., Pan, D., and Pan, D. (2017). Paper-based analytical biosensor chip designed from graphene-nanoplatelet-amphiphilic-diblock-co-polymer composite for cortisol detection in human saliva. *Anal. Chem.* **89**, 2107–2115.
39. Oster, H., Challet, E., Ott, V., Arvat, E., de Kloet, E.R., Dijk, D.J., Lightman, S., Vgontzas, A., and Van Cauter, E. (2016). The functional and clinical significance of the 24-h rhythm of circulating glucocorticoids. *Endocr. Rev.* **38**, 3–45.
40. Laudat, M.H., Cerdas, S., Fournier, C., Guiban, D., Guilhaume, B., and Luton, J.P. (1988). Salivary cortisol measurement: a practical approach to assess pituitary-adrenal function. *J. Clin. Endocrinol. Metab.* **66**, 343–348.
41. Ivars, K., Nelson, N., Theodorsson, A., Theodorsson, E., Ström, J.O., and Mörelius, E. (2015). Development of salivary cortisol circadian rhythm and reference intervals in full-term infants. *PLoS One* **10**, e0129502.
42. Russell, E., Koren, G., Rieder, M., and Uum, S.H.M.V. (2013). The detection of cortisol in human sweat. *Ther. Drug Monit.* **36**, 30–34.
43. Katchman, B.A., Zhu, M., Christen, J.B., and Anderson, K.S. (2018). Eccrine sweat as a biofluid for profiling immune biomarkers. *Proteom. Clin. Appl.* **12**, 1800010.
44. Burke, P.M., Reichler, R.J., Smith, E., Dugaw, K., McCauley, E., and Mitchell, J. (1985). Correlation between serum and salivary cortisol levels in depressed and nondepressed children and adolescents. *Am. J. Psychiatry* **142**, 1065–1067.
45. Vanbruggen, M.D., Hackney, A.C., McMurray, R.G., and Ondrak, K.S. (2011). The relationship between serum and salivary cortisol levels in response to different intensities of exercise. *Int. J. Sports Physiol. Perform.* **6**, 396–407.
46. Jung, C., Greco, S., Nguyen, H.H., Ho, J.T., Lewis, J.G., Torpy, D.J., and Inder, W.J. (2014). Plasma, salivary and urinary cortisol levels following physiological and stress doses of hydrocortisone in normal volunteers. *BMC Endocr. Disord.* **14**, 91.
47. Dickerson, S.S., and Kemeny, M.E. (2004). Acute stressors and cortisol responses: a theoretical integration and synthesis of laboratory research. *Psychol. Bull.* **130**, 355–391.
48. Kudielka, B.M., and Wüst, S. (2010). Human models in acute and chronic stress: assessing determinants of individual hypothalamus–pituitary–adrenal axis activity and reactivity. *Stress* **13**, 1–14.
49. Kanaley, J.A. (2001). Cortisol and growth hormone responses to exercise at different times of day. *J. Clin. Endocrinol. Metab.* **86**, 2881–2889.
50. Weise, M., Drinkard, B., Mehlinger, S.L., Holzer, S.M., Eisenhofer, G., Charmandari, E., Chrousos, G.P., and Merke, D.P. (2004). Stress dose of hydrocortisone is not beneficial in patients with classic congenital adrenal hyperplasia undergoing short-term, high-intensity exercise. *J. Clin. Endocrinol. Metab.* **89**, 3679–3684.
51. Luger, A., Deuster, P.A., Kyle, S.B., Gallucci, W.T., Montgomery, L.C., Gold, P.W., Loriaux, D.L., and Chrousos, G.P. (1987). Acute hypothalamic-pituitary-adrenal responses to the stress of treadmill exercise. *N. Engl. J. Med.* **316**, 1309–1315.
52. Rimmele, U., Zellweger, B.C., Marti, B., Seiler, R., Mohiyeddini, C., Ehler, U., and Heinrichs, M. (2007). Trained men show lower cortisol, heart rate and psychological responses to psychosocial stress compared with untrained men. *Psychoneuroendocrinology* **32**, 627–635.
53. Thuma, J.R., Gilders, R., Verdun, M., and Loucks, A.B. (1995). Circadian rhythm of cortisol confounds cortisol responses to exercise: implications for future research. *J. Appl. Physiol.* **78**, 1657–1664.
54. Schwabe, L., Haddad, L., and Schachinger, H. (2008). HPA axis activation by a socially evaluated cold-pressor test. *Psychoneuroendocrinology* **33**, 890–895.
55. Zimmer, C., Basler, H.-D., Vedder, H., and Lautenbacher, S. (2003). Sex differences in cortisol response to noxious stress. *Clin. J. Pain* **19**, 233–239.
56. Goodin, B.R., Smith, M.T., Quinn, N.B., King, C.D., and McGuire, L. (2012). Poor sleep quality and exaggerated salivary cortisol reactivity to the cold pressor task predict greater acute pain severity in a non-clinical sample. *Biol. Psychol.* **91**, 36–41.
57. Mcrae, A.L., Saladin, M.E., Brady, K.T., Upadhyaya, H., Back, S.E., and Timmerman, M.A. (2006). Stress reactivity: biological and subjective responses to the cold pressor and Trier Social stressors. *Hum. Psychopharmacol.* **21**, 377–385.
58. Bullinger, M., Naber, D., Pickar, D., Cohen, R.M., Kalin, N.H., Pert, A., and Bunney, W.E., Jr. (1984). Endocrine effects of the cold pressor test: relationships to subjective pain appraisal and coping. *Psychiatry Res.* **12**, 227–233.
59. Geliebter, A., Gibson, C.D., Hernandez, D.B., Atalayer, D., Kwon, A., Lee, M.I., Mehta, N., Phair, D., and Gluck, M.E. (2012). Plasma cortisol levels in response to a cold pressor test did not predict appetite or ad libitum test meal intake in obese women. *Appetite* **59**, 956–959.
60. Mitchell, L.A., Macdonald, R.A., and Brodie, E.E. (2004). Temperature and the cold pressor test. *J. Pain* **5**, 233–237.
61. Machale, S., Cavanagh, J.T., Bennie, J., Carroll, S., Goodwin, G.M., and Lawrie, S.M. (1998). Diurnal variation of adrenocortical activity in chronic fatigue syndrome. *Neuropsychobiology* **38**, 213–217.
62. Strickland, P., Morriss, R., Wearden, A., and Deakin, B. (1998). A comparison of salivary cortisol in chronic fatigue syndrome, community depression and healthy controls. *J. Affect. Disord.* **47**, 191–194.
63. Vythilingam, M., Gill, J.M., Luckenbaugh, D.A., Gold, P.W., Collin, C., Bonne, O., Plumb, K., Polignano, E., West, K., and Charney, D. (2010). Low early morning plasma cortisol in posttraumatic stress disorder is associated with co-morbid depression but not with enhanced glucocorticoid feedback inhibition. *Psychoneuroendocrinology* **35**, 442–450.